Journal of Zhejiang University-SCIENCE A in press
www.jzus.zju.edu.cn; www.springer.com/journal/11582
E-mail: jzus_a@zju.edu.cn

Research Article
https://doi.org/10.1631/jzus.A2500239

Impact of heterogeneous electrode design on vanadium redox flow batteries with different flow fields

Jie SUN[1], Menglian ZHENG[2,3]✉, Mengxin YU[1], Jinbo CHEN[1], Jianxin LI[1], Changxing HU[1]

[1] *Institute of Energy and Environment Engineering, NingboTech University, Ningbo, 315100, China*
[2] *Institute of Thermal Science and Power Systems, School of Energy Engineering, Zhejiang University, Hangzhou, 310027, China*
[3] *State Key Laboratory of Clean Energy Utilization, Hangzhou, 310027, China*

Abstract: With the rapid progress of processing technology, the heterogeneous optimization design of porous electrodes is becoming practicable. Nevertheless, there is currently a lack of understanding of the relevant theoretical foundation. In this study, we systematically examined the influence and mechanism of various carbon paper stacking schemes on the performance of vanadium redox flow batteries (VRFBs) with different flow fields (interdigitated flow field, IFF, and serpentine flow field, SFF) through experiments and simulations. We found that the optimization of porous electrode heterogenization showed significant differences. For the IFF, optimizing the porous electrode structure remarkably improved the mass transfer effect near the membrane, thus enhancing the performance of VRFBs. For the SFF, the effectiveness of electrode structure optimization was manifested mainly in improvement of the permeability of the porous electrode. Furthermore, the effectiveness of the heterogeneous design of the porous electrode depended on a balanced relationship between the mass transfer rate of the reactants and the rate of the electrochemical reaction. The Damköhler number was introduced to measure this balance and serve as a basis for subsequent optimization.

Key words: VRFB; Serpentine flow field; Interdigitated flow field; Heterogeneous electrode design; Carbon paper; Damköhler number

1 Introduction

Vanadium redox flow batteries (VRFBs) represent a promising electrochemical energy storage technology due to their long cycle life, quick response, high reliability, and absence of electrolyte cross-contamination (Ye et al., 2024; Gautam and Kumar, 2022; Ye et al., 2024). To promote the large-scale industrialization of VRFBs, research has focused on improving their power density to reduce system costs (Huynh et al., 2025; Zarei-Jelyani et al., 2023; Huang et al., 2022). The porous electrode, which not only provides active sites for redox reactions, but also affects the ion and mass transport within it, plays a crucial role in reducing the high polarization in VRFBs (Wang et al., 2024; He et al., 2022). In addition to using various pretreatment methods to improve the surface activity of the porous electrode (Ye et al., 2022), enhancing its structural design can optimize its performance (Ye et al., 2024; Forner-Cuenca and Brushett, 2019). Since changes in the pore structure of the electrode can also lead to alterations in the specific surface area, structural optimization often results in the coupled refinement of its mass transfer - electrochemical process (Lv et al., 2024).

Electrode structure optimization generally can be either homogeneous or heterogeneous. This classification is based on whether there is overall consistency or local differences in the porous structure of the electrode (Wan et al., 2021; Alphonse et al., 2023). Given that the electrochemical reaction occurs nonlinearly in the electrode and reactants are non-uniformly distributed from the inlet to the outlet, heterogeneous optimization is more intricate. It often produces better results in balancing the mass transfer property and specific surface area. For instance, Hu et al. (Hu et al., 2018) reported a hybrid electrode composed of graphene oxide for enhanced reactivity

✉ Menglian ZHENG, menglian_zheng@zju.edu.cn
Menglian ZHENG, https://orcid.org/0000-0002-4418-4361

Received June 8, 2025; Revision accepted Oct. 22, 2025;
Crosschecked

and reduced graphene foam for improved conductivity. This electrode significantly reduces battery polarization, thereby enhancing the charge and discharge capacity and efficiency. Jiang et al. (Jiang et al., 2019; Jiang et al., 2019) and Chen et al. (Chen et al., 2019) proposed novel electrode structures with gradient or double-layered porous media from the bipolar plate side to the membrane side. These structures aim to balance the requirements of sufficient mass transport and a high specific surface area in the flow cell, resulting in a lower charge voltage and a higher discharge voltage for VRFBs. Research by Yoon et al. (Yoon et al., 2019) showed that optimizing the porosity distribution in the in-plane direction of the porous electrode to match the reactants' concentration distribution is also crucial for increasing the power density and energy efficiency of the flow cell without a flow field design. Thus, carrying out heterogeneous and sophisticated optimization design on porous electrodes is an effective approach to enhance the power density of VRFBs.

The non-uniform distribution of reactant transfer and electrochemical reactions within the porous electrode provides a practical foundation and rationale for its heterogeneous optimization design (Zeng et al., 2023; Mukhopadhyay et al., 2019). This non-uniform distribution is closely associated with the flow field structure, which is an essential factor that should not be overlooked during the optimization process (Huang et al., 2021; Pezeshki et al., 2017). For example, Pezeshki et al. (Pezeshki et al., 2017) and Maurya et al. (Maurya et al., 2018) both discovered that the performance of flow cells using different electrode materials is closely related to the type of flow fields. In the case of a flow cell with a serpentine flow field (SFF), the mass transfer overpotential in carbon paper electrodes is significantly higher than that of carbon felt (Duan et al., 2022; Wang et al., 2022). However, for a flow cell with equal path length flow fields (EPL), this drawback has been eliminated (Houser et al., 2017). Houser et al. (Houser et al., 2016) found that increasing the number of layers of carbon paper electrodes can significantly reduce the mass transfer overpotential of the flow cell with SFF. In contrast, for a flow cell with an interdigitated flow field (IFF), the influence of the number of layers of carbon paper is not significant. Therefore, we conclude that during the optimization design process of porous electrodes, the influence of flow fields should be fully considered (Muñoz-Perales et al., 2023).

Carbon paper is thin and has a high specific surface area. Its stacked use was first proposed in the zero-gap design (Maurya et al., 2018). Previous studies have shown that this method can significantly enhance the power density and energy efficiency of VRFBs. However, the underlying basis of its enhanced performance still requires in-depth understanding. Although previous research has explored heterogeneous electrodes by layering different numbers and types of carbon paper, it remains unclear how the structure of layered electrodes, in combination with flow field designs, improves the reactant concentration and thereby the overpotential distribution. Therefore, in this study, we aimed to address the question of how to conduct heterogeneous optimization design of porous electrodes for flow cells implemented with different flow fields. Given their extensive applications, we focused on two types of flow fields: IFF and SFF. Moreover, based on our previous findings, the non-uniformity of mass transfer and electrochemical reactions occurs mainly in the through-plane direction of the electrode under these two flow fields (Sun et al., 2019). Thus, we focused mainly on heterogeneous optimization design of the porous electrode in this direction. Two representative carbon paper electrodes (SGL39AA and SGL38AA) were combined to form a single electrode for heterogeneous design.

The remainder of this paper is structured as follows. First, Section 2 details the design of the heterogeneous electrode for the flow cell. Section 3 describes the experimental and simulation methods used in this study. In Section 4, we present and discuss the experimental and simulation results of different heterogeneous electrode designs for VRFBs implemented with different flow fields. Finally, Section 5 presents the conclusions and future research directions.

2 Approaches

2.1 Combined electrode design for VRFBs with IFF or SFF

Two different carbon papers (SGL39AA and SGL38AA) were used. Their typical physical properties (Table 1) were supplied by the manufacturer (SGL Carbon Group, Germany) or experimentally determined. The pore diameter of 39AA (42-44 um) is larger than that of 38AA (25-29 um), therefore its porosity (81%) and permeability (11-12E10-12 m2) are also higher than those of 38AA (75%, 3-4E10-12 m2), but the corresponding specific surface area of 39AA (173000 m-1) is smaller than that of 38AA (412000 m-1). Note that a higher specific surface area typically corresponds to smaller and more densely distributed pores within the electrode, which in turn reduces its permeability. Consequently, these two properties show an inverse, trade-off relationship, and the performance of a porous electrode fundamentally depends on the balance between the mass transfer rate of reactants and the rate of electrochemical reactions.

Regardless of whether it is IFF or SFF, the flow paths between adjacent tributaries are U-shaped (Fig. 1) (Sun et al., 2023). The main distinction between IFFs and SFFs lies in their overall structure: in an SFF, the inlet and outlet are directly connected, whereas in an IFF, they are not. This structural difference determines whether the process of electrolyte penetration into the porous electrode is active or passive. Specifically, in an IFF, the electrolyte will fully penetrate the electrode, while in SFF, the amount of electrolyte penetrating the electrode depends on the pressure difference between adjacent flow channels and the flow resistance along the U-shaped flow paths (Sun et al., 2022). Our preliminary research indicated that the electrolyte velocity and reactant concentration are strongly correlated with the flow path. This implies that an optimal heterogeneous optimization design should take the flow path as an important reference. Nevertheless, considering the constraints of practical manufacturing, we carried out heterogeneous optimization only in the thickness direction. The complete electrode consisted of three layers of carbon paper, in six different combinations (Fig. 1(c)).

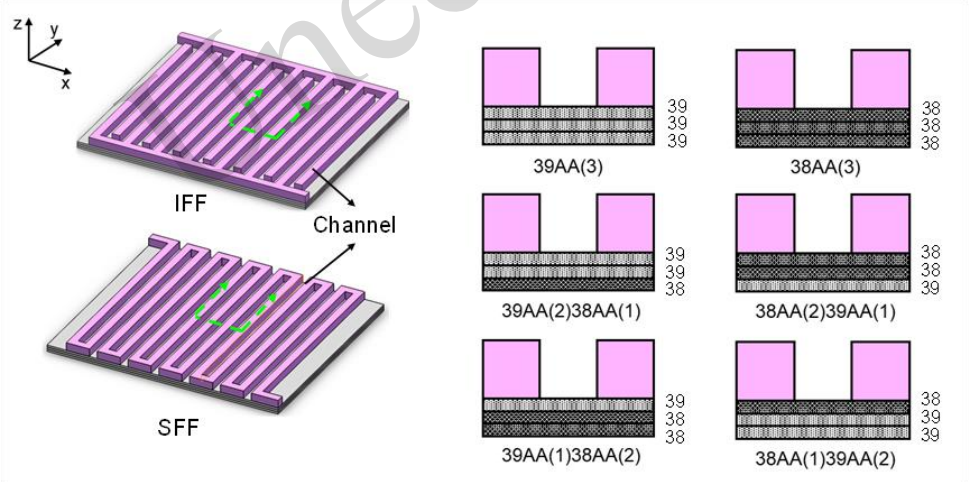

Fig. 1 Combined electrode design for a VRFB with IFF or SFF. They are named according to the top-down order and number of layers

Table 1 Typical properties of SGL39AA and SGL38AA carbon paper

Typical properties	SGL39AA	SGL38AA
Thickness # [μm]	280	280
Porosity* [%]	81	75
Mean pore diameter # [μm]	42-44	25-29
Electric conductivity # [S·cm-1]	5	5
Permeability # [10-12m2]	11-12	3-4
Specific surface area* [m-1]	173000	412000

*Experimentally determined, #provided by the manufacturer.

2.2 Experimental methods

VRFB single flow cell system

Our experiments were conducted on a VRFB single flow cell system. In the flow cell, the positive and negative SGL® carbon paper electrodes are separated by a Nafion® 117 membrane, and the

bipolar plates machined with the flow field are made from graphite composite material (Beijing Jinglong Special Carbon Industrial Co., Ltd.). Two peristaltic pumps (Masterflex®, L/S 07525-40) were used to cycle the electrolyte (1.6 M vanadyl sulfate dissolved in 4 M sulfuric acid solutions, Dalian BR New Material Co.).

IR-corrected polarization curve tests

The polarization curves were taken at 0.5 SOC and different flow rates of 5 mL/min and 20 mL/min. The two different flow rates represent two distinct operational states in VRFBs: mass transfer-limited and mass transfer-unlimited conditions (see Section 4.2a for a more detailed discussion). To ensure the consistency of SOC during each polarization test, we first used a dedicated VRFB to charge a large volume of electrolyte under constant current conditions for a predetermined duration. The charging duration was determined by charge conservation. Besides, we ensured that the open-circuit equilibrium voltage remained consistent prior to each polarization test. During the measurement, each side used two tanks so that the electrolyte passed through the cell only once without circulation, thereby maintaining a constant electrolyte concentration for the tests. The polarization curves were obtained under potentiostatic control from an open circuit voltage (OCV) of 1.4 to 0 V. In addition, the high frequency resistance of the cell was measured under 20 kHz to correct the ohmic loss of the cell for the polarization curves. A Bio-Logic® VSP electrochemical workstation was used for the above tests. Fig. 2 shows the structure of the experimental system.

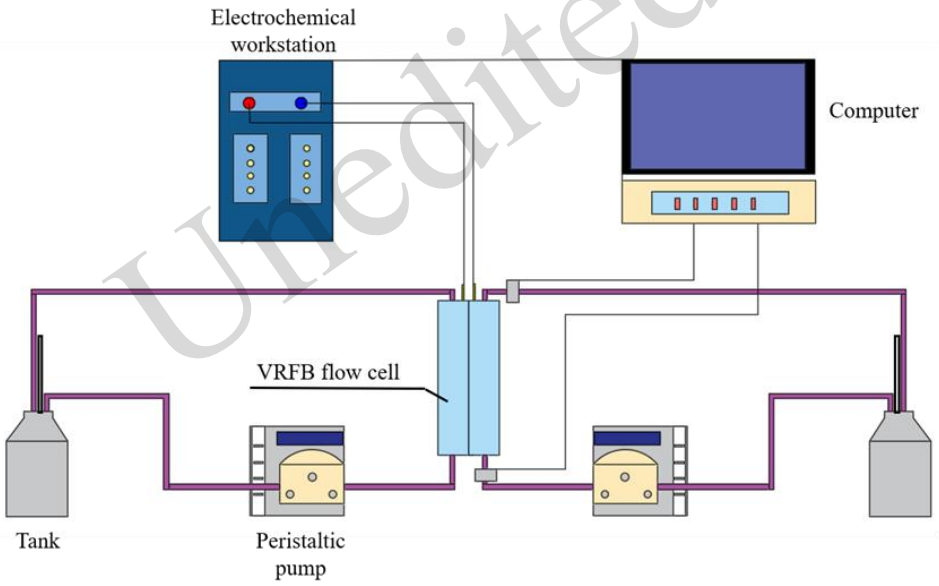

Fig. 2 Experimental system diagram.

2.3 Simulation methods

To obtain a more in-depth analysis of how the heterogeneous porous electrode affects the performance of the flow cell, we developed a three-dimensional, multi-physical model with the use of COMSOL Multiphysics®, which can simulate the mass transfer and electrochemical reaction processes in the flow cell. The detailed modelling process (including geometry, governing equations, boundary conditions, and initial values, relevant parameters for the specific battery configuration, and the numerical method) has been published (Sun et al., 2019). The model used in this study used different carbon paper electrodes, as described in Section 2.1, and was validated (see Supplementary Material).

3 Results

3.1 Performance of combined electrode for a VRFB with IFF

First, we conducted experimental tests to examine the impact of using a combination electrode on the polarization performance of a VRFB with an IFF (Fig. 3). When only one layer of carbon paper was used as the electrode, we observed that the

performance of 38AA was better than that of 39AA, achieving a 25% increase in the limiting current density (Fig. (3a)). We attribute this mainly to the larger specific surface area of 38AA, which facilitates an increase in the volumetric mass transfer rate and a reduction in the overpotential within the porous electrode. When the number of electrode layers increased from 1 to 3, although the performance of the VRFB using either 38AA or 39AA as electrodes improved, the increase in the limiting current density achieved by 39AA was significantly greater. The limiting current density of the 39AA electrode increased by about 50% compared to that of the single-layer 39AA electrode, an increase so great that that the difference between the two electrodes was negligible in the case of three-layer electrodes. An increase in the number of electrode layers has opposing effects: on the one hand, it enlarges the total reaction area, which is conducive to enhancing the peak current density. On the other hand, the overall increase in electrode thickness leads to a rise in the resistance overpotential. Moreover, the expansion of the overall electrode volume gives rise to more significant unevenness in mass transfer and electrochemical reactions, thereby restricting further improvement of the limiting current density. The enhanced performance of the 3-layer 39AA was better than that of the 3-layer 38AA. This indirectly confirmed that the unevenness introduced by 38AA was more pronounced, which might be associated with the low permeability of 38AA, as it impedes the rapid and uniform transfer of ions.

We performed simulations to further elucidate the experimental observations. When there was only one layer of carbon paper electrode, the distribution of the electrolyte flow rate among the two types of carbon paper electrodes was identical (Fig. (3b)). Nevertheless, owing to the difference in specific surface area, there was a notable disparity in the overpotential. When the number of electrode layers was increased to three, the electrolyte flow rate distribution in the electrode composed of 39AA was more uniform, thereby avoiding large localized mass transfer overpotentials (Fig. 3(c)). This compensates for the adverse effect of insufficient specific surface area and is comparable to the overall overpotential of 38AA. Consequently, we conclude that in IFF VRFBs, the high permeability of 39AA results in low flow resistance, making it more suitable for applications where mass transfer is the limiting factor. In contrast, the high specific surface area of 38AA leads to low electrochemical reaction resistance, making it more appropriate for scenarios with favorable mass transfer conditions.

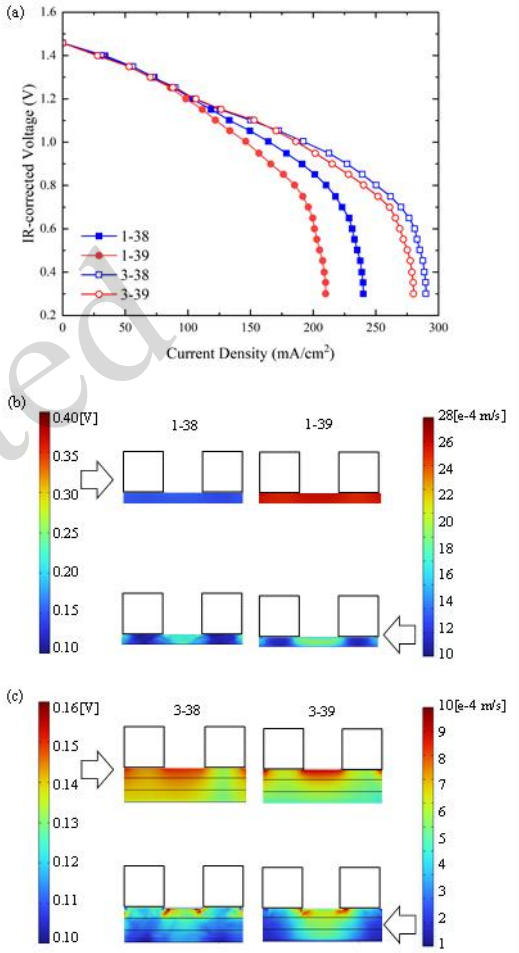

Fig. 3 (a) IR-corrected polarization curves of the VRFB flow cell with the IFF and electrodes made of carbon paper with different numbers of layers and types. (b) Distribution of overpotential and electrolyte flow velocity in the 1-layer carbon paper electrode obtained through simulation. (c) Distribution of overpotential and electrolyte flow velocity in the 3-layer carbon paper electrode obtained through simulation. Testing was based on a flow rate of 5 mL/min.

In the porous electrode consisting of three layers of 38AA, the poor permeability of 38AA caused a lower flow rate of the electrolyte near the membrane side, thereby resulting in poor mass transfer (Fig. 3(c)). Consequently, we propose replacing the layer

of 38AA adjacent to the membrane side with 39AA while maintaining the other two layers as 38AA to leverage its high reactive specific surface area. Thus, the composition of the porous electrode from the bipolar plate side to the membrane side is 38AA - 38AA - 39AA (i.e., higher porosity near the membrane). Moreover, to demonstrate the effects, we also examined the electrode with the reverse composition (39 - 38 - 38).

We observed that in comparison to the three-layer electrode composed solely of 38AA or 39AA carbon paper, the 38-38-39 combination enhanced the limiting current density of the VRFBs by about 17% (Fig. 4(a)). Conversely, the 39-38-38 combination reduced it by around 20%. Furthermore, according to the simulation results, the efficacy of the 38-38-39 combination stems from two main aspects. Firstly, as mentioned above, the higher permeability of 39AA results in reduced flow resistance on the near-membrane side, thereby facilitating a greater distribution of electrolyte to this region. Therefore, positioning 39AA on the side adjacent to the membrane significantly enhances mass transfer in the vicinity. Secondly, placing 38AA in a region with superior mass transfer (the side near the bipolar plate) offers sufficient specific surface area for the reaction. These two factors jointly enhance the electrochemical performance of the VRFB. In contrast, for the 39-38-38 combination, 38AA exacerbates the deterioration of mass transfer in the near-membrane region. Although 39AA increases the electrolyte flow rate near the bipolar plate side, it fails to provide adequate specific surface area, ultimately leading to a substantial decline in the electrochemical performance of the VRFBs.

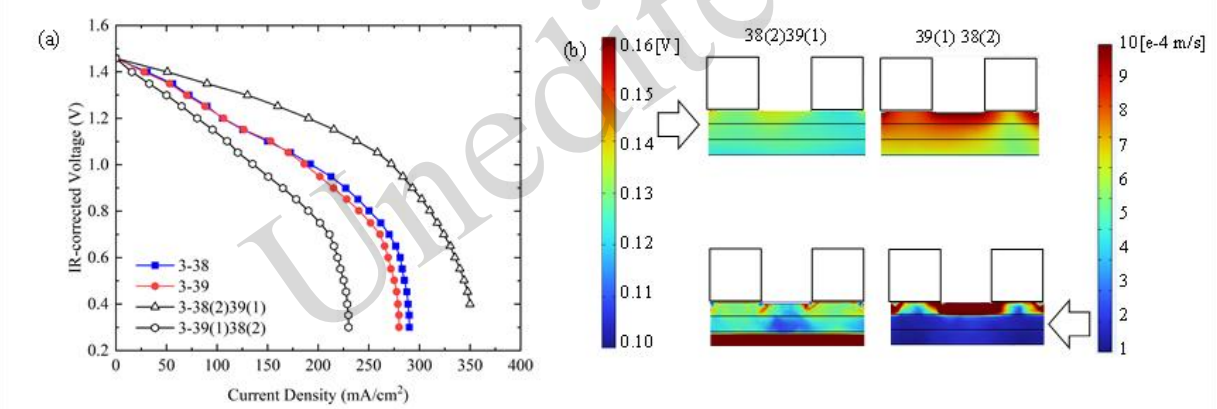

Fig. 4 (a) IR-corrected polarization curves of the VRFB flow cell with the IFF and electrodes made of carbon paper with three layers and different combinations. (b) Distribution of overpotential and electrolyte flow velocity in the 3-layer carbon paper electrode obtained through simulation. Testing was based on a flow rate of 5 mL/min.

3.2 Performance of combined electrode for a VRFB with SFF

Although using the same electrode combination, VRFBs with the SFF or IFF exhibited notable differences in performance. As depicted in Fig. 5(a), when the electrode was composed of a single type of carbon paper, regardless of whether it was one or three layers, the performance of the SFF was inferior to that of the IFF. Specifically, the limiting current density of the SFF was generally 20-60% lower. We attribute this difference to the structural characteristics of the SFF and the resulting fluid dynamics. The SFF features a fully connected flow path from the inlet to the outlet, which implies that the electrolyte may bypass the porous electrode without fully penetrating it before exiting the VRFB. Consequently, the extent of electrolyte penetration into the porous electrode is governed by the flow resistance, or permeability, of the electrode itself. In contrast, the IFF consists of two isolated flow domains, requiring the electrolyte to fully traverse the porous electrode before exiting the system. Therefore, under certain conditions, the degree of electrolyte penetration in SFF VRFBs is necessarily lower than that in IFF VRFBs. Reduced electrolyte penetration typically corresponds to a lower electrolyte velocity within the porous electrode, which ultimately results in reduced polarization performance.

Another aspect worthy of attention is that in VRFBs with the SFF, although 38AA carbon paper has a larger specific surface area, this advantage did not evidently enhance the performance of VRFBs. In contrast, 39AA consistently demonstrated better performance. With one layer of carbon paper, 39AA led to a 25% increase in the limiting current density, which rose to 65% when three layers of carbon paper were stacked. The permeability and average pore size of 38AA are considerably smaller than those of 39AA. This leads to a higher flow resistance, which restricts the penetration of the electrolyte into the porous electrode and ultimately limits the electrochemical performance of the VRFB (details are provided in Table S1 of the Supplementary Materials). The velocity distributions shown in Fig. 5(b) and (c) provide a partial explanation for the phenomena. Owing to the limited penetration of the electrolyte, the flow velocity of the electrolyte within the electrode is significantly lower, while the corresponding overpotential loss is substantial. We conclude that for VRFBs using the SFF, the permeability of the porous electrode is a crucial indicator, followed by the specific surface area.

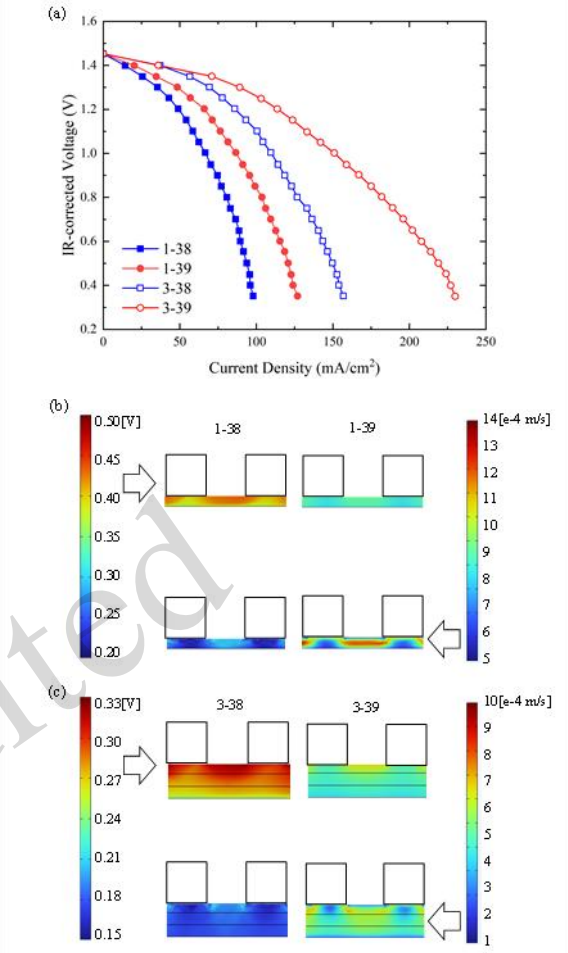

Fig. 5 (a) IR-corrected polarization curves of the VRFB flow cell with the SFF and electrodes made of carbon paper with different layers and types. (b) Distribution of overpotential and electrolyte flow velocity in a 1-layer carbon paper electrode obtained through simulation. (c) Distribution of overpotential and electrolyte flow velocity in the 3-layer carbon paper electrode obtained through simulation. Testing was based on a flow rate of 5 mL/min.

For VRFBs using the SFF, when attempting to use electrodes formed by the combination of 38AA and 39AA, the resulting effect differed significantly. The performance of the composite electrode was superior to that of the electrode composed solely of 38AA (with an approximate 15% increase in the limiting current density), yet inferior to that of the electrode composed solely of 39AA (with an approximate 25% reduction in the limiting current density) (Fig. 6(a)). This result aligns with our previous inference. That is, for VRFBs using SFF, the permeability of the porous electrode is the most crucial factor, followed by the specific surface area

of the porous electrode. Whether it is the 39-38-38 combination or the 38-38-39 combination, both contain a layer of 39AA electrodes. Therefore, compared to electrodes composed of three layers of 38AA, the combined electrodes achieved a certain degree of enhanced permeability, but they still did not match the performance of electrodes composed of three layers of 39AA. Regarding the 38-38-39 combination, its performance was slightly better than that of the 39-38-38 combination, but still fell within the scope of the discussion regarding the complementary advantages of mass transfer and electrochemistry. Specifically, the 38-38-39 combination places the highly permeable 39AA in an area with originally poor mass transfer, while the 39-38-38 combination places the 39AA with a low specific surface area in an area with originally good mass transfer. Clearly, the distribution strategy of the 38-38-39 combination is better.

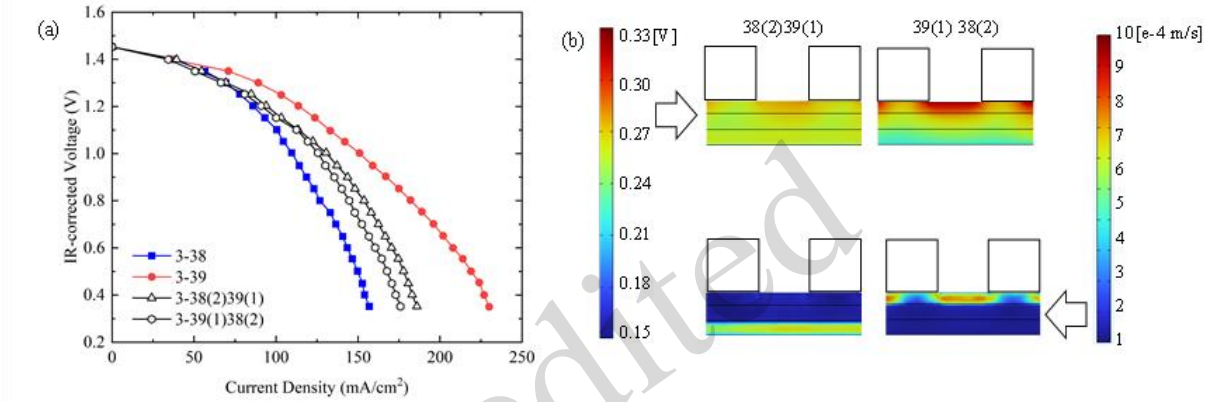

Fig. 6 (a) IR-corrected polarization curves of the VRFB flow cell with the SFF and electrodes made of carbon paper with three layers and different combinations. (b) Distribution of overpotential and electrolyte flow velocity in the 3-layer carbon paper electrode obtained through simulation. Testing was based on a flow rate of 5 mL/min.

4 Discussion

4.1 Dimensionless parameters describing the effectiveness of porous electrodes

The efficacy of this heterogeneous optimization of the porous electrode hinges on the balanced relationship between the mass transfer rate of the reactants and the rate of the electrochemical reaction. We can use the Damköhler number to measure this balance and serve as a basis for subsequent optimization.

$$Da^* = \frac{T_{\mathrm{mt}}}{T_{\mathrm{rea}}} = \frac{k_{\mathrm{rea}} \cdot a \cdot L^2}{k_{\mathrm{mt}}}$$

where, T_{mt} is the characteristic time of reactant transport; T_{rea} is the characteristic time of the electrochemical reaction; k_{rea} is the electrochemical reaction rate constant, and k_{mt} is the effective mass transfer coefficient of the diffusion layer (note that during the calculation process, we averaged both k_{rea} and k_{mt} across the entire computational domain. Furthermore, as our previous research (Zheng et al., 2024) indicated that k_{rea} is associated mainly with the modification of the reaction surface and shows minimal correlation with electrode structural parameters or battery operational conditions, it was not explicitly discussed in the subsequent analysis of the results). a is the specific surface area of the porous electrode, and L is the characteristic length of reactant transport, which is taken as the thickness of porous electrode. When $Da^* \gg 1$, the system performance is limited by mass transfer. Extensive research has indicated that in VRFBs, the mass transfer process is significantly slower than the electrochemical reaction process and serves as the main limiting factor. Thus, enhancing the material transport process within porous electrodes is of crucial significance. Fig. 7 depicts the electrolyte flow velocity, the effective mass transfer coefficient of the diffusion layer, and the Damköhler number in the porous electrodes of the VRFBs with the IFF or SFF.

For the VRFB with the IFF, the 38-38-39 combination had the highest electrolyte velocity, the most efficient transfer coefficient, and the smallest Damköhler number. This finding aligns with the

optimal polarization curve discussed in Section 3.1. Note that higher flow rates do not necessarily correspond to larger effective mass transfer coefficients. For instance, although the 39-39-39 combination had a higher velocity than the 38-38-38 combination, its effective mass transfer coefficient was lower. This is because the effective mass transfer coefficient is not solely dependent on velocity but is also affected by microscopic factors such as pore diameter and specific surface area. On the other hand, for the VRFB with the SFF, the 39-39-39 combination had the highest velocity and effective transfer coefficient, along with the smallest Damköhler number, which is consistent with the findings in Section 3.2. Meanwhile, due to the poor permeability of carbon paper, the overall electrolyte velocity of the VRFB with the SFF was low, the effective mass transfer coefficient was small, and the Damköhler number was relatively large. Consequently, this led to its overall subpar performance. In summary, the Damkohler number is directly correlated with the polarization performance of VRFBs. The heterogeneous design of porous electrodes effectively balances the relative rates of mass transfer and electrochemical reactions, thereby minimizing the Damkohler number and consequently improving VRFBs performance. This insight offers a more reliable theoretical foundation for future optimization of porous electrode structures.

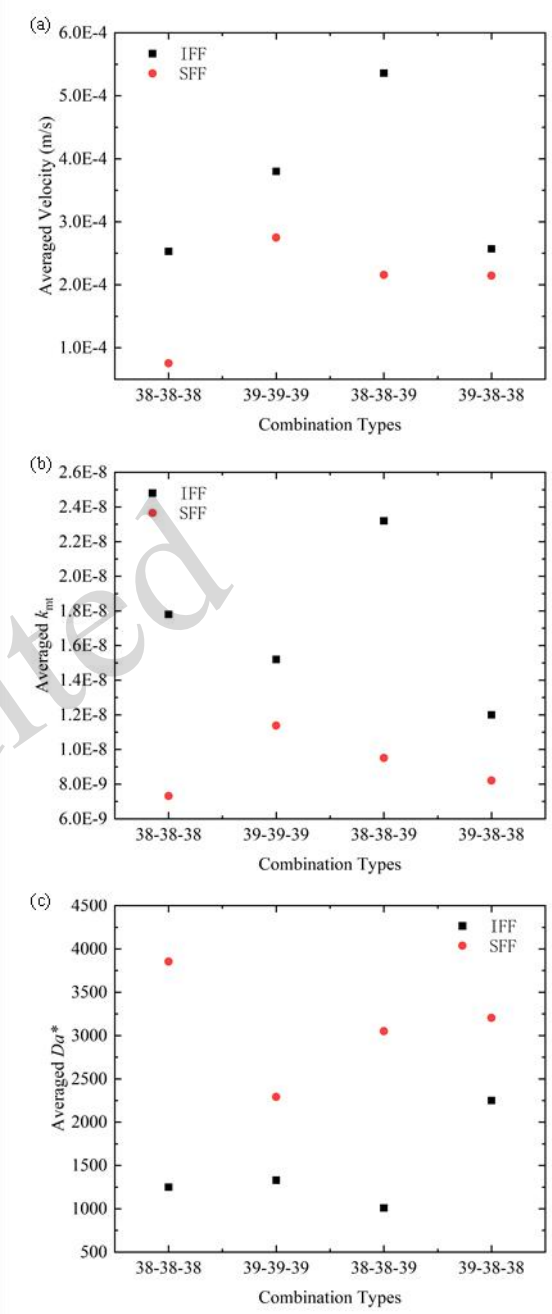

Fig. 7 (a) Averaged velocity, (b) effective mass transfer coefficient, and (c) Damköhler number in the 3-layer carbon paper electrode obtained through simulation. Testing was based on a flow rate of 5 mL/min.

4.2 Effects of the inlet flow rate

The polarization curve presented in Section 3 shows a pronounced drop, indicating that the related analysis is applicable exclusively to the mass transfer-limited regime. Considering the alterations in the inlet flow rate of the VRFB, which directly

influence the electrolyte velocity within the porous electrode and the effective mass transfer coefficient in the diffusion layer, ultimately affecting Da*, we experimentally examined the polarization curves of the VRFB using the IFF and SFF at higher flow rates and mass transfer-unlimited conditions. As shown in Fig. 8(a) and (b), an increase in the inlet flow rate had a certain positive effect on both the IFF and SFF. However, the performance improvement of the VRFB using the IFF was more notable (the value of the critical current density nearly doubled). This is because the augmented inlet flow can be fully manifested as an enhanced electrolyte velocity in the porous electrode, ultimately reducing Da*. For the SFF, although an increased flow rate can facilitate the penetration of the electrolyte into the electrodes, its impact is restricted. Additionally, when the flow rate is increased, the polarization performance of the 38-38-38 combination for the VRFB using IFF surpassed that of the 38-38-39 combination. This is because the flow rate within the porous electrode is sufficiently high at this stage to counteract the adverse effects of poor mass transfer near the membrane side, ultimately attaining the lowest Da* value.

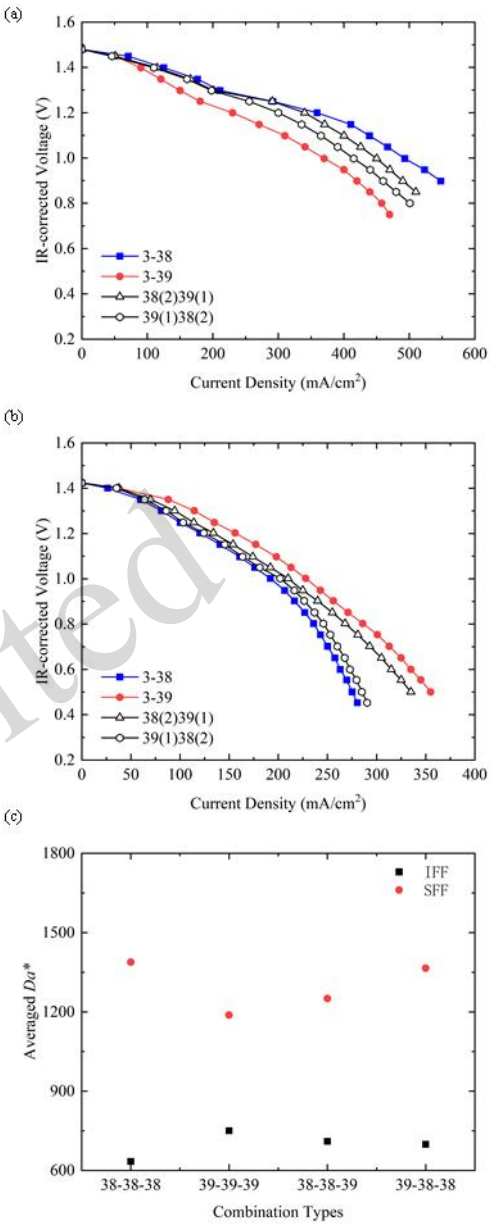

Fig. 8 IR-corrected polarization curves of the VRFB flow cell with (a) IFF and (b) SFF, and (c) corresponding Damköhler numbers, at an inlet flow rate of 20 mL/min.

4.3 Effects of the types of electrodes

Given the significant differences between carbon paper (CP) and graphite felt (GF) porous electrodes in terms of pore diameter, specific surface area, and permeability, we investigated their different effects on the IFF and SFF. The order of the channel and porous electrode combinations from highest to lowest performance was respectively:

IFF-CP>SFF-GF>SFF-CP>IFF-GF. This order aligns with the corresponding Da* trend. Note that, in general, the permeability of graphite felt was one to two orders of magnitude higher than that of carbon paper. When graphite felt was used as the electrode material, the performance of the SFF was markedly superior to that of the IFF, further highlighting the significance of electrode permeability in SFF applications

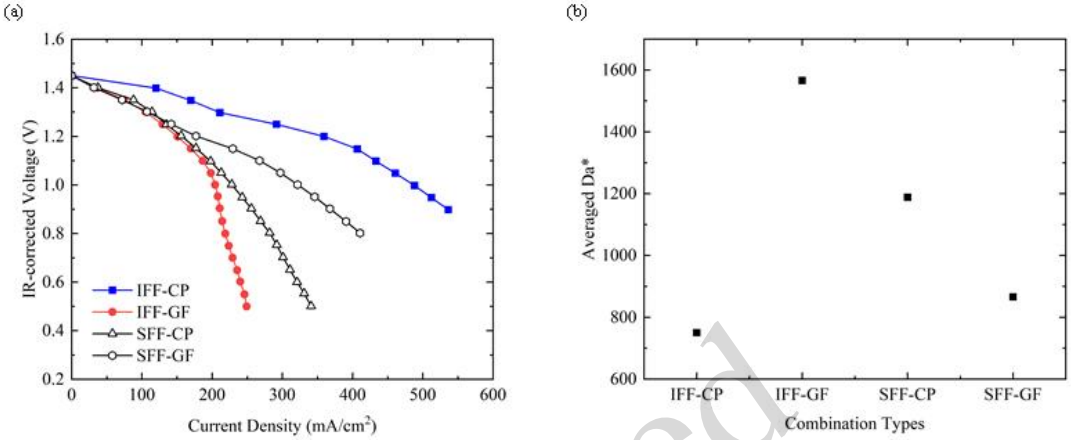

Fig. 9 (a) IR-corrected polarization curves of the VRFB flow cell with different flow fields and porous electrodes based on an inlet flow rate of 5 mL/min, and (b) corresponding Damköhler numbers. CP represents a porous electrode composed of three layers of carbon paper, while GF represents a graphite felt porous electrode. The thickness of the different electrodes was maintained at the same magnitude.

4.4 Future work

After a series of studies, we found that although heterogeneous electrode design had a significant effect on the IFF, its effect on the SFF was very small. In this context, we have formulated preliminary concepts concerning the heterogeneous design of porous electrodes for the SFF. Given that the electrolyte flow within the SFF structure may induce concentration variations along the in-plane direction of the electrode, implementing a heterogeneous design along this axis could yield more substantial performance enhancements. Nevertheless, due to practical limitations in the fabrication of porous electrodes with such designs, this line of research has not yet been fully realized. Advanced manufacturing techniques such as 3-D printing may enable complex heterogeneous designs along the in-plane direction in the future.

5 Conclusions

We undertook a systematic and comprehensive study of the heterogeneous optimization of porous electrodes in VRFBs with different flow fields, using both experimental and simulation approaches. The main findings were as follows:

1. For VRFBs using the IFF, the heterogeneous design of porous electrodes has a notable influence. Owing to the poor mass transfer resulting from the low electrolyte flow velocity near the membrane side of the porous electrode, adopting a structure with a higher porosity at this location is often effective.

2. For VRFBs adopting the SFF, since the flow field fails to compel all the electrolyte to penetrate the porous electrode, ensuring the permeability of the porous electrode becomes the primary objective, aiming to guarantee the penetration flow rate and mass transfer efficiency of the electrolyte within the porous electrode. Nevertheless, the optimization design of heterogeneity has a limited impact.

3. Furthermore, the effectiveness of the porous electrode depends on a balanced relationship between the mass transfer rate of the reactants and the rate of the electrochemical reaction. We introduced the Damköhler number to quantify this balance and serve as a basis for subsequent optimization. The validity of this parameter was verified under different combinations of channels and electrodes.

Acknowledgments

This work was supported by the Zhejiang Provincial Natural Science Foundation of China [grant number LQ23E060003], the Ningbo Municipal Natural Science Foundation of China [grant number 2023J398], the Fundamental Research Funds for the Central Universities [grant number 2022ZFJH004], and the Ningbo Natural Science Foundation [grant number 2023J276].

Author contributions

Jie SUN and Menglian ZHENG designed the research. Jie SUN and Mengxin YU processed the corresponding data. Jie SUN wrote the first draft of the manuscript. Menglian ZHENG helped to organize the manuscript. Jianxin LI and Jinbo CHEN and Changxing Hu revised and edited the final version.

Conflict of interest

Jie SUN, Menglian ZHENG, Mengxin YU, Jinbo CHEN, Jianxin LI, and Changxing HU declare that they have no conflict of interest.

References

Ye L, Qi S, Cheng T, et al., 2024. Vanadium redox flow battery: review and perspective of 3D electrodes. *ACS Nano*, 18(29): 18852-18869. https://doi.org/10.1021/acsnano.4c06675

Gautam RK, Kumar A, 2022. A review of bipolar plate materials and flow field designs in the all-vanadium redox flow battery. *Journal of Energy Storage*, 48: 104003. https://doi.org/10.1016/j.est.2022.104003

Ye J, Xia L, Li H, et al., 2024. The critical analysis of membranes toward sustainable and efficient vanadium redox flow batteries. *Advanced Materials*, 36(28): 2402090. https://doi.org/10.1002/adma.202402090

Huynh TTK, Yang T, PS N, et al.,2025. Construction of High-Performance Membranes for Vanadium Redox Flow Batteries: Challenges, Development, and Perspectives. *Nano-Micro Letters*, 17(1): 260. https://doi.org/10.1007/s40820-025-01736-x

Zarei-Jelyani M, Loghavi MM, Babaiee M, et al., 2023. The significance of charge and discharge current densities in the performance of vanadium redox flow battery. *Electrochimica Acta*, 443: 141922. https://doi.org/10.1016/j.electacta.2023.141922

Huang Z, Mu A, Wu L, et al., 2022. Comprehensive analysis of critical issues in all-vanadium redox flow battery. *ACS sustainable chemistry & engineering*, 10(24): 7786-7810. https://doi.org/10.1021/acssuschemeng.2c01372

Wang P, Zhao Y, Ban Y, et al., 2024. A review of porous electrode structural parameters and optimization for redox flow batteries. *Journal of Energy Storage*, 97: 112859. https://doi.org/10.1016/j.est.2024.112859

He Z, Lv Y, Zhang T, et al., 2022. Electrode materials for vanadium redox flow batteries: Intrinsic treatment and introducing catalyst. *Chemical Engineering Journal*, 427: 131680. https://doi.org/10.1016/j.cej.2021.131680

Ye J, Zheng C, Liu J, et al., 2022. In situ grown tungsten trioxide nanoparticles on graphene oxide nanosheet to regulate ion selectivity of membrane for high performance vanadium redox flow battery. *Advanced Functional Materials*, 32(8): 2109427. https://doi.org/10.1002/adfm.202109427

Ye L, Qi S, Cheng T, et al., 2024. Vanadium redox flow battery: review and perspective of 3D electrodes. *ACS nano*, 18(29): 18852-18869. https://doi.org/10.1021/acsnano.4c06675

Forner-Cuenca A, Brushett FR, 2019. Engineering porous electrodes for next-generation redox flow batteries: recent progress and opportunities. *Current Opinion in Electrochemistry*, 18: 113-122. https://doi.org/10.1016/j.coelec.2019.11.002

Lv W, Luo Y, Xu Y, et al., 2024. Laser perforated porous electrodes in conjunction with interdigitated flow field for mass transfer enhancement in redox flow battery. *International Journal of Heat and Mass Transfer*, 224: 125313. https://doi.org/10.1016/j.ijheatmasstransfer.2024.125313

Wan S, Liang X, Jiang H, et al., 2021. A coupled machine learning and genetic algorithm approach to the design of porous electrodes for redox flow batteries. *Applied Energy*, 298: 117177. https://doi.org/10.1016/j.apenergy.2021.117177

Alphonse PJ, Taş M, Elden G, 2023. Novel electrode design having gradually increasing porosity in a vanadium redox flow battery. *Fuel*, 333: 126198. https://doi.org/10.1016/j.fuel.2022.126198

Hu G, Jing M, Wang DW, et al., 2018. A gradient bi-functional graphene-based modified electrode for vanadium redox flow batteries. *Energy Storage Materials*, 13: 66-71. https://doi.org/10.1016/j.ensm.2017.12.026

Jiang HR, Zhang B W, Sun J, et al., 2019. A gradient porous electrode with balanced transport properties and active surface areas for vanadium redox flow batteries. J*ournal of Power Sources*, 440: 227159. https://doi.org/10.1016/j.jpowsour.2019.227159

Jiang HR, Shyy W, Wu MC, et al., 2019. A bi-porous graphite felt electrode with enhanced surface area and catalytic activity for vanadium redox flow batteries. *Applied Energy*, 233: 105-113. https://doi.org/10.1016/j.apenergy.2018.10.033

Chen W, Kang J, Shu Q, et al., 2019. Analysis of storage capacity and energy conversion on the performance of gradient and double-layered porous electrode in all-vanadium redox flow batteries. *Energy*, 180: 341-355. https://doi.org/10.1016/j.energy.2019.05.037

Yoon S J, Kim S, Kim DK, 2019. Optimization of local porosity in the electrode as an advanced channel for all-vanadium redox flow battery. *Energy*, 172: 26-35. https://doi.org/10.1016/j.energy.2019.01.101

Zeng C, Kim S, Chen Y, et al., 2023. In situ characterization of kinetics, mass transfer, and active electrode surface area

for vanadium redox flow batteries. *Journal of The Electrochemical Society*, 170(3): 030507. https://doi.org/10.1149/1945-7111/acbf7f

Mukhopadhyay A, Yang Y, Li Y, et al., 2019. Mass transfer and reaction kinetic enhanced electrode for high-performance aqueous flow batteries. *Advanced Functional Materials*, 29(43): 1903192. https://doi.org/10.1002/adfm.201903192

Huang Z, Mu A, Wu L, et al., 2022. Vanadium redox flow batteries: Flow field design and flow rate optimization. *Journal of Energy Storage*, 45: 103526.

Huang Z, Mu A, 2021. Flow field design and performance analysis of vanadium redox flow battery. *Ionics*, 27: 5207-5218. https://doi.org/10.1016/j.est.2021.103526

Pezeshki AM, Sacci RL, Delnick FM, et al., 2017. Elucidating effects of cell architecture, electrode material, and solution composition on overpotentials in redox flow batteries. *Electrochimica Acta*, 229: 261-270. https://doi.org/10.1016/j.electacta.2017.01.056

Maurya S, Nguyen PT, Kim YS, et al., 2018. Effect of flow field geometry on operating current density, capacity and performance of vanadium redox flow battery. *Journal of Power Sources*, 404: 20-27. https://doi.org/10.1016/j.jpowsour.2018.09.093

Duan ZN, Zhang GB, Zhang JF, et al., 2022. Experimental Investigation on the Performance Characteristics of Flow Fields in Redox Flow Batteries Under Various Electrode Parameters. *Frontiers in Thermal Engineering*, 2: 931160. https://doi.org/10.3389/fther.2022.931160

Wang Y, Li M, Hao L, 2022. Three-dimensional modeling study of all-vanadium redox flow batteries with the serpentine and interdigitated flow fields. Journal of Electroanalytical Chemistry, 918: 116460. https://doi.org/10.1016/j.jelechem.2022.116460

Houser J, Pezeshki A, Clement JT, et al., 2017. Architecture for improved mass transport and system performance in redox flow batteries. *Journal of Power Sources*, 351: 96-105. https://doi.org/10.1016/j.jpowsour.2017.03.083

Houser J, Clement J, Pezeshki A, et al., 2016. Influence of architecture and material properties on vanadium redox flow battery performance. *Journal of Power Sources*, 302: 369-377. https://doi.org/10.1016/j.jpowsour.2015.09.095

Muñoz-Perales V, García-Salaberri PÁ, Mularczyk A, et al., 2023. Investigating the coupled influence of flow fields and porous electrodes on redox flow battery performance. *Journal of Power Sources*, 586: 233420. https://doi.org/10.1016/j.jpowsour.2023.233420

Maurya S, Nguyen PT, Kim YS, et al., 2018. Effect of flow field geometry on operating current density, capacity and performance of vanadium redox flow battery. *Journal of Power Sources*, 404: 20-27. https://doi.org/10.1016/j.jpowsour.2018.09.093

Sun J, Zheng M, Luo Y, et al., 2019. Three-dimensional detached serpentine flow field design for redox flow batteries. *Journal of Power Sources*, 428: 136-145. https://doi.org/10.1016/j.jpowsour.2019.04.106

Sun J, Luo Y, Zheng M, et al., 202. An analytical model for parametric study on serpentine and interdigitated flow fields in redox flow batteries. *Journal of Energy Storage*, 71: 108188. https://doi.org/10.1016/j.est.2023.108188

Sun J, Liu B, Zheng M, et al., 2022. Serpentine flow field with changing rib width for enhancing electrolyte penetration uniformity in redox flow batteries. *Journal of Energy Storage*, 49: 104135. https://doi.org/10.1016/j.est.2022.104135

Sun J, Zheng M, Yang Z, et al., 2019. Flow field design pathways from lab-scale toward large-scale flow batteries. *Energy*, 173: 637-646. https://doi.org/10.1016/j.energy.2019.02.107

Zheng M, Liu K, Sun J, et al., 2024. Quantifying effects of surface morphology and functional groups of carbon fibers on mass transfer coefficient in vanadium redox flow batteries. *Energy*, 291: 130237. https://doi.org/10.1016/j.energy.2024.130237

Electronic supplementary materials

Table S1, Figs. S1–S2

中文概要

题　目： 非均质化多孔电极结构对采用不同流道结构的液流电池的影响研究

作　者： 孙洁[1]，郑梦莲[2,3]，余梦馨[1]，陈金波[1]，李建新[1]，胡长兴[1]

机　构： [1]浙大宁波理工学院，能源与环境系统工程研究所，中国宁波，315100；[2]浙江大学，能源工程学院，热工与动力系统研究所，中国杭州，310027；[3]能源清洁利用国家重点实验室，中国杭州，310027

目　的： 传质与电化学反应分布不均是限制全钒液流电池功率密度和充放电效率的关键瓶颈。本文旨在通过对多孔电极进行非均质化的优化设计，改进不同流道结构下全钒液流电池的传质和电化学反应效率，以提高电池性能。

创新点： 1. 针对采用不同流道结构的全钒液流电池，分别提出了相应的电极非均质化优化设计方案；2. 引入无量纲参数，为多孔电极非均质化设计提供理论依据。

方　法：1. 通过仿真模拟，深入分析了多孔电极非均质化优化对电池过电位损失的作用机制；3. 通过实验测试，验证了多孔电极非均质化优化对液流电池性能提升的有效性。

结　论：1. 对于采用交叉型流道的全钒液流电池，多孔电极的非均质化设计具有显著影响。由于靠近膜侧的多孔电极附近电解液流速低导致传质不良，因此在该位置采用孔隙率更高的结构通常较为有效；2. 对于采用 蛇型流道的全钒液流电池而言，由于流场无法迫使所有电解液穿透多孔电极，确保多孔电极的渗透性成为首要目标，旨在保证电解液在多孔电极内的渗透流速和传质效率。在这种情况下，多孔电极非均质化的优化设计影响有限；3. 多孔电极的有效性取决于反应物的质量传递速率与电化学反应速率之间的平衡关系。我们引入了达姆科勒数来量化这种平衡，并将其作为后续优化的基础。在不同通道和电极组合的情况下，对该参数的有效性进行了验证。

关键词：液流电池；蛇型流道；交叉型流道；非均质化多孔电极设计；碳纸；Da 数